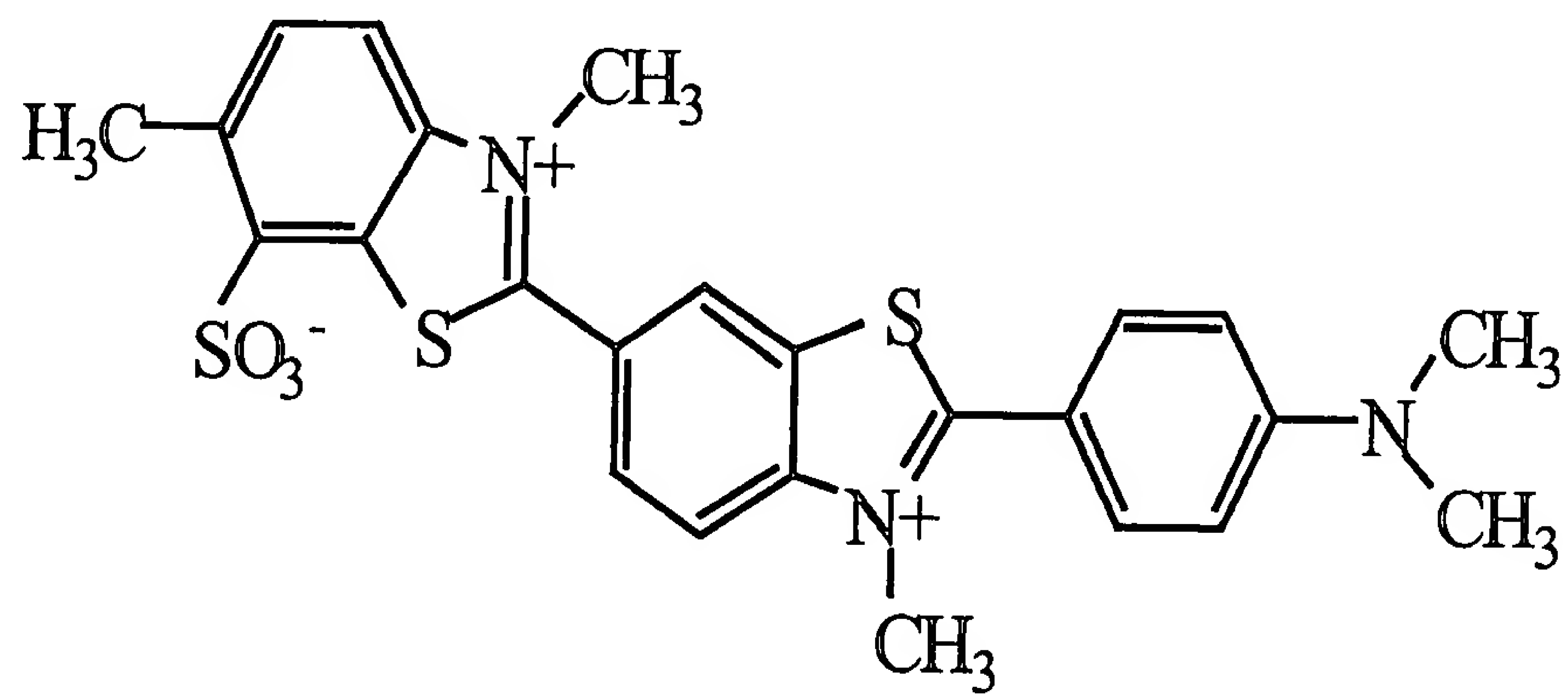

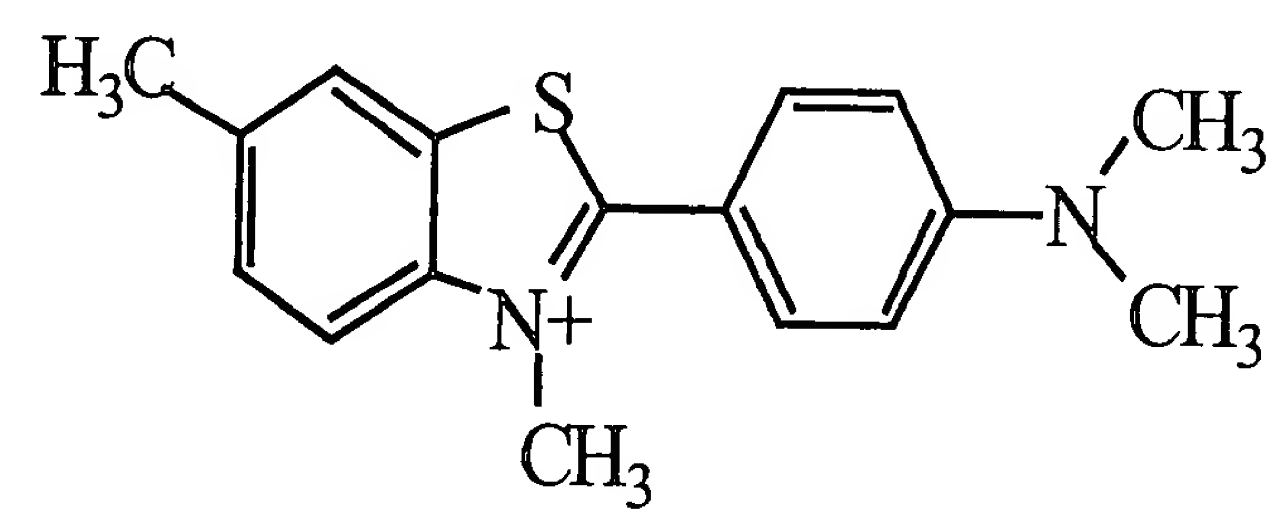

Thioflavin T (ThT)

Proposed Structure of a Major Component of Thioflavin S (ThS)

Figure 1. Structures of a major component of the mixture that comprises Thioflavin S and the chemically well-defined compound, Thioflavin T.

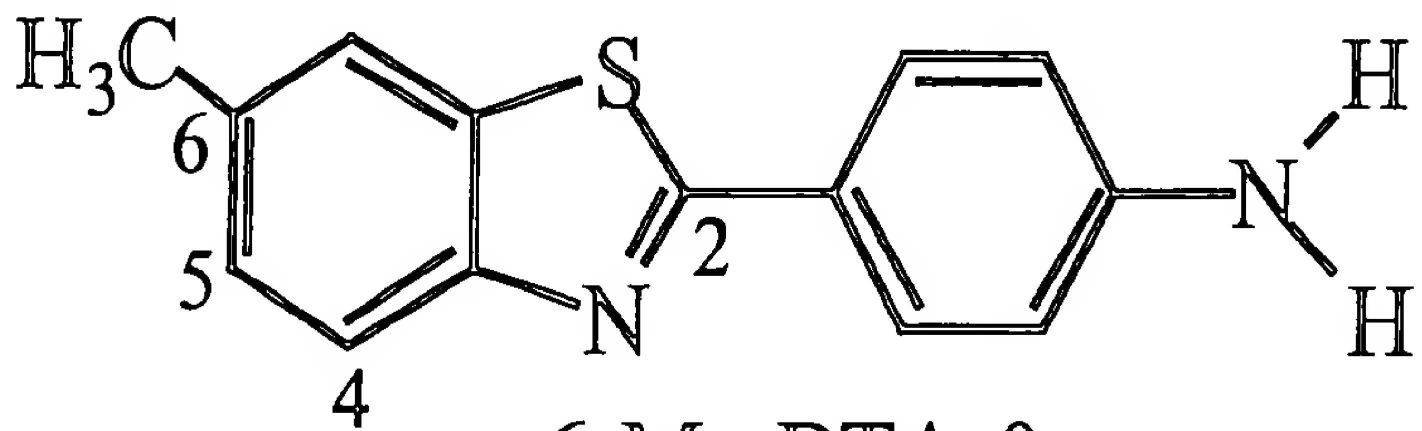

6-Me-BTA-0

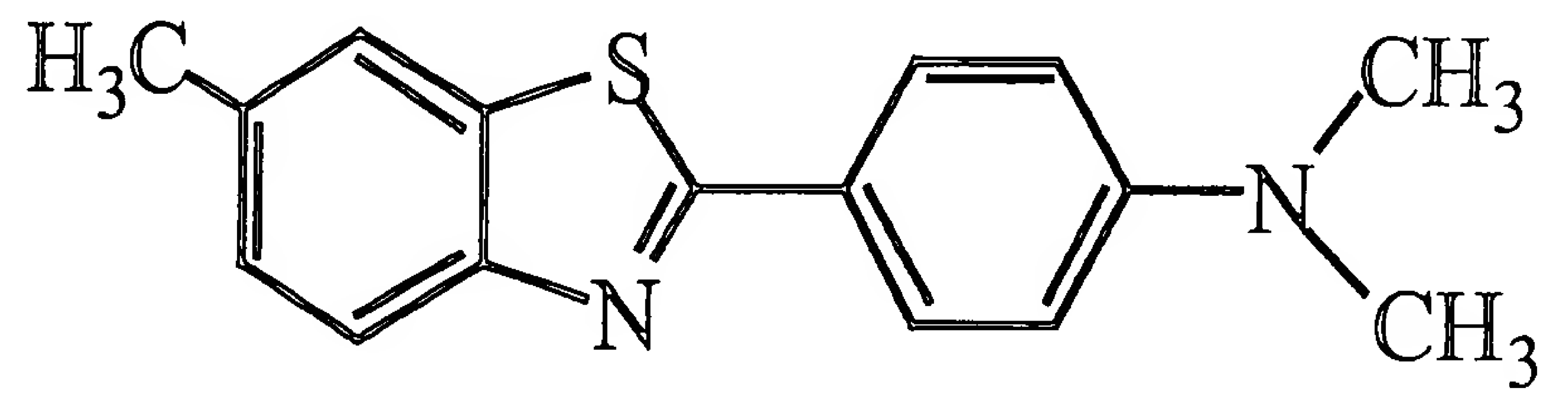

6-Me-BTA-2

Figure 2. Structures of two Thioflavin T analogs in which the quaternary amine of the benzthioazole ring has been replaced with an uncharged tertiary amine.

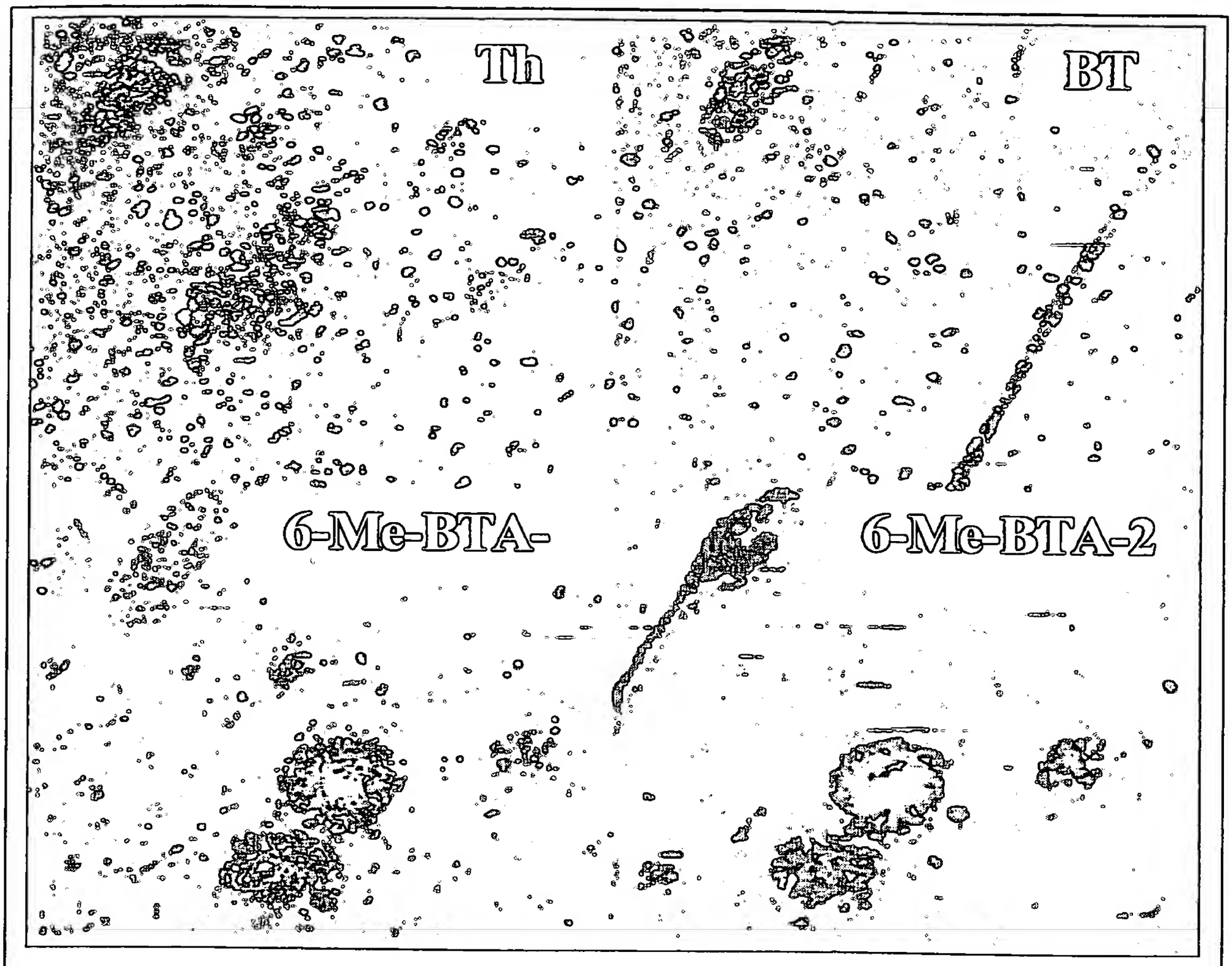

Figure 3. Four serial sections of AD brain frontal cortex stained with the fluorescent dye ThT and three derivatives of ThT are shown. The arrow indicates the same vessel in each section for orientation. Three large amyloid plaques in the mid-lower to right quadrant of each panel are seen clearly with the 6-Me-BTA-0 and 6-Me-BTA-2 stains and are not visualized as well with ThT and BTP stains.

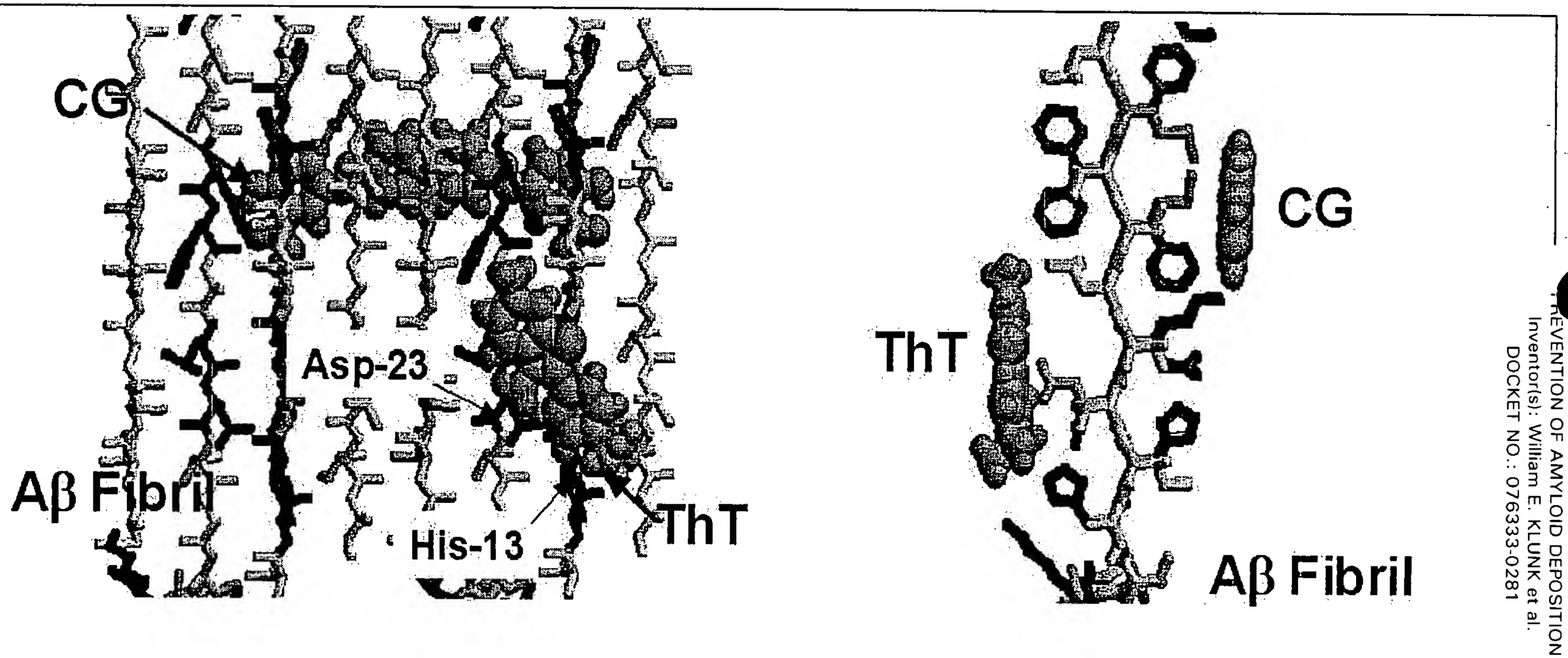

Figure 4. Proposed sites of Chrysamine G and Thioflavin T binding to a hypothetical β-sheet fibril. (left) ThT and CG may bind to the Aβ fibril on opposite sides. CG may bind to Glu-22/Lys-16, while ThT may bind to Asp-23/His-13. (right) Right angle view of the left panel, showing ThT and CG binding on opposite sides of the Aβ fibril.

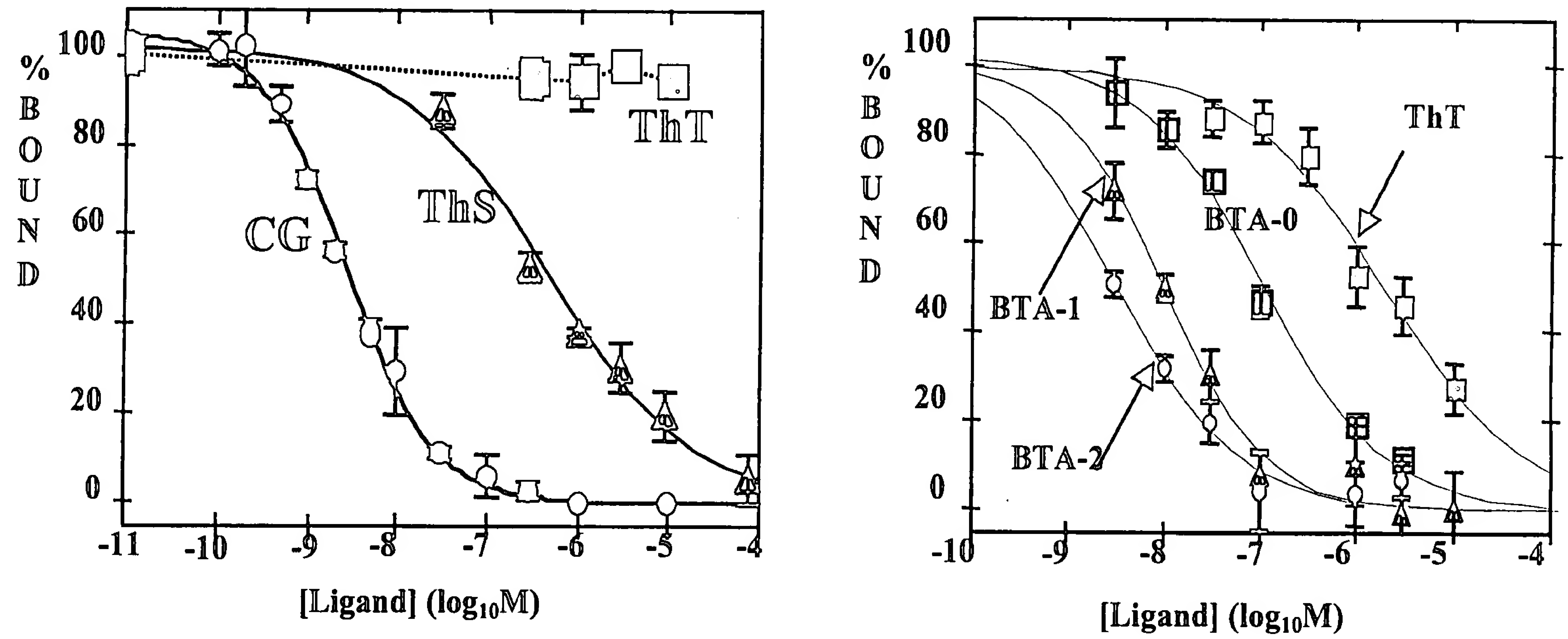

Figure 5. (left) Competition assay using [^{3}H]CG and Aβ(1-40) fibrils. While Thioflavin S competed with a lower affinity than CG for binding sites, Thioflavin T did not inhibit [^{3}H]CG binding even at 10 μM concentrations. (right) Competition binding assays of ThT analogs using [N-methyl-^{11}C]-BTA-1 and Aβ(1-40) fibrils. All of the BTA derivatives were more potent competitors than ThT.

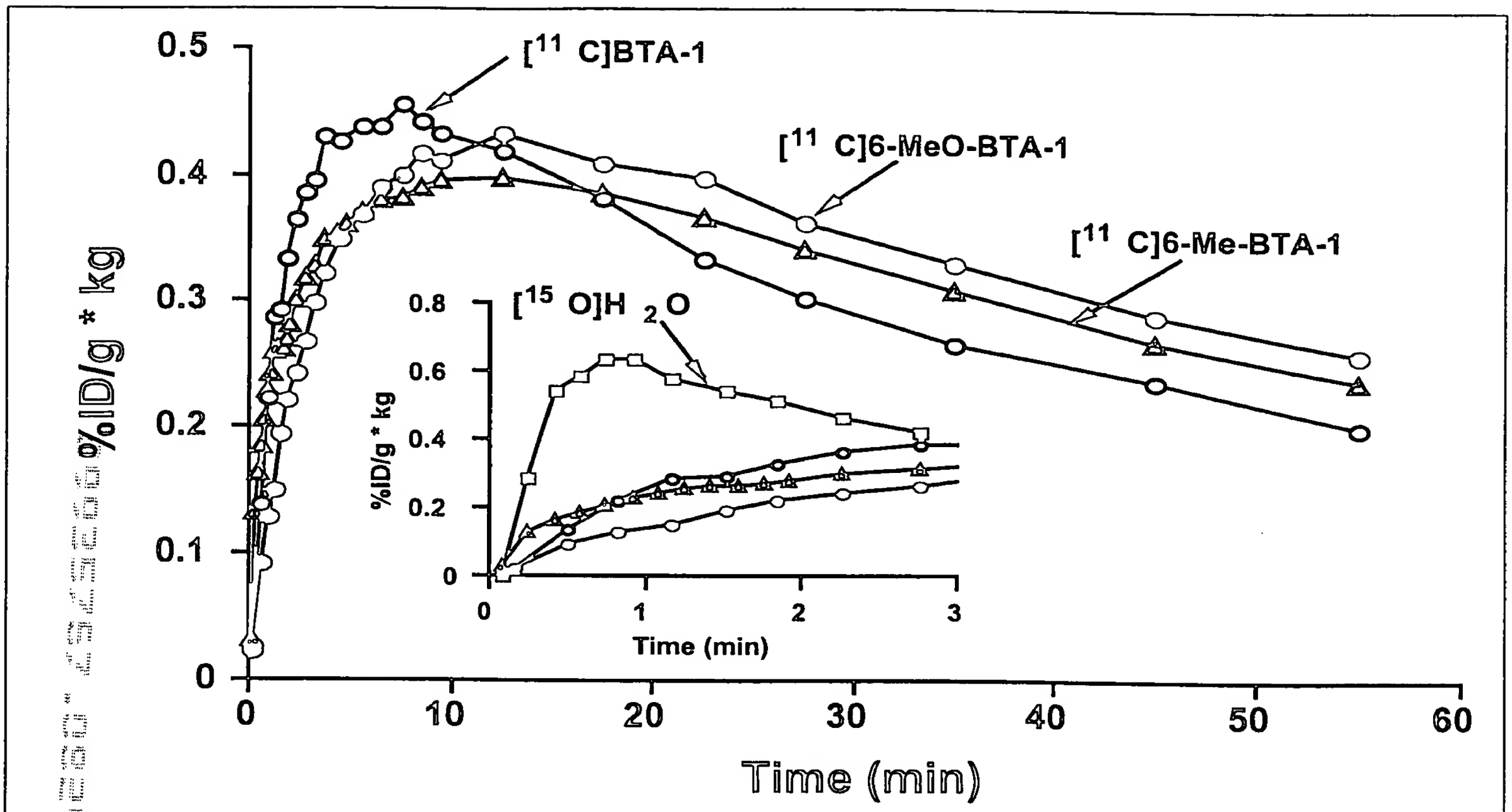

Figure 6. Time course of radioactivity in the frontal cortex of baboons injected intravenously with 3-5 mCi of ^{11}C-labeled BTA-1, 6-MeO-BTA-1, or 6-Me-BTA-1. Other brain regions, including cerebellum, provided nearly identical time-activity curves indicating a lack of regional uptake preference for the radiotracers in normal brain tissues (see Fig. 7). The smaller inset figure shows the uptake of tracers in the frontal cortex at early time points following injection relative to the blood flow tracer [^{15}O]water.

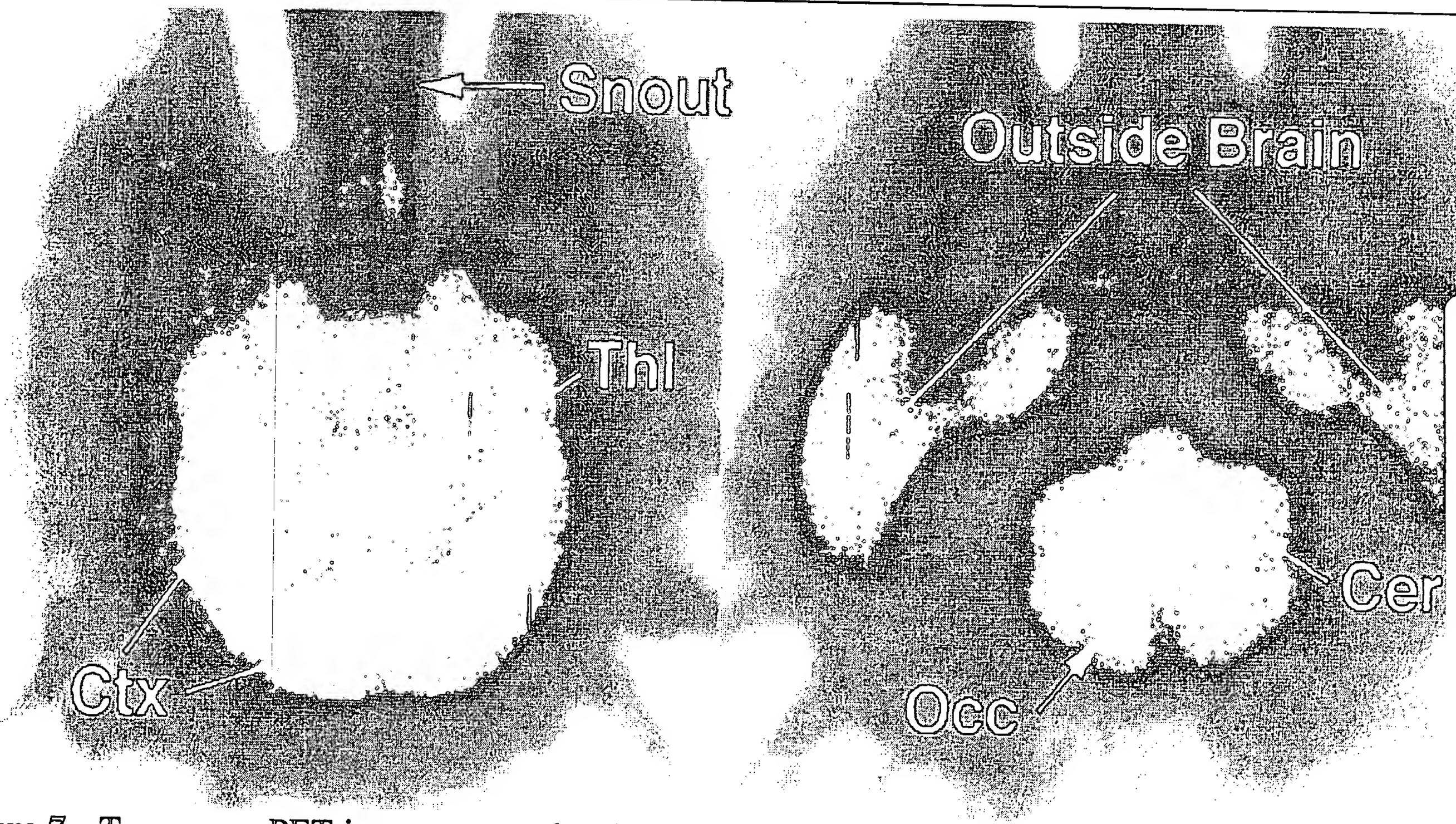

Figure 7. Transverse PET images at two levels of baboon brain following the i.v. injection of 3 mCi of [N-methyl-^{11}C]BTA-1

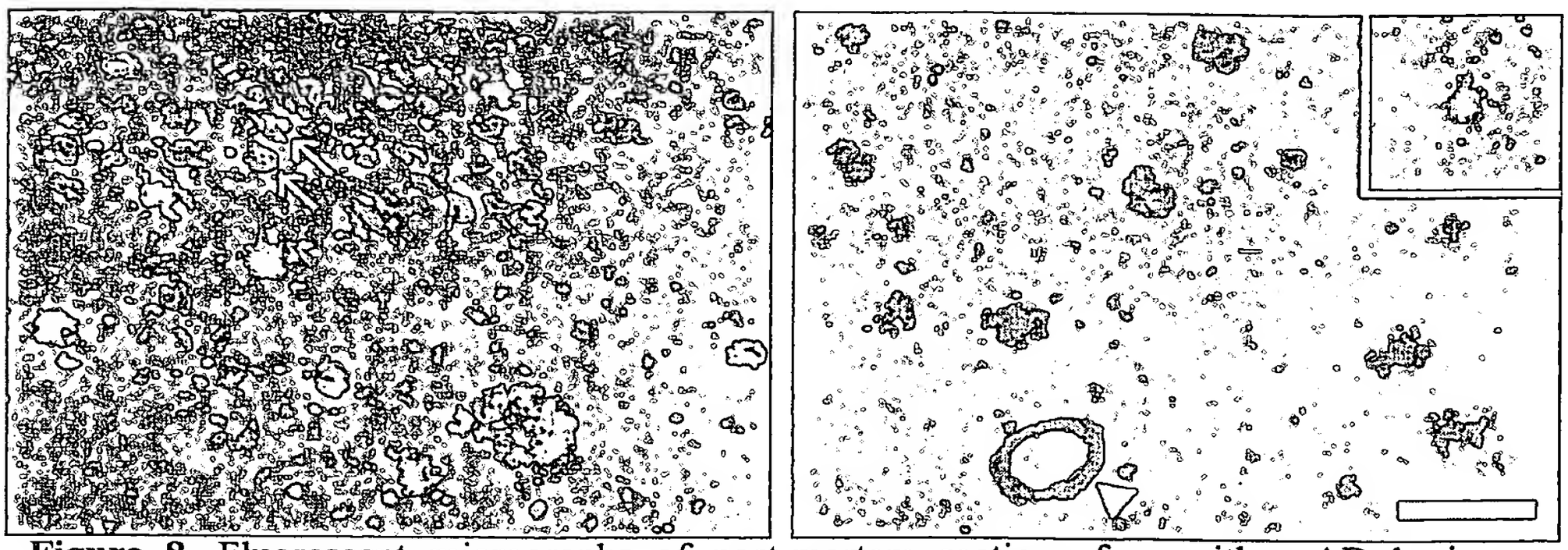

Figure 8. Fluorescent micrographs of post-mortem sections from either AD brain or PS1/APP transgenic mouse brain (inset) stained with BTA-1. *Left:* AD entorhinal cortex showing many NFT in the upper half (two are marked by arrows) and several plaques in the lower half. *Right:* AD frontal cortex showing several plaques and the cross-section of a blood vessel laden with amyloid (arrowhead). *Inset:* A single amyloid plaque in the cortex of an 8 month-old PS1/APP mouse. The scale bar represents 100 μm in all micrographs.

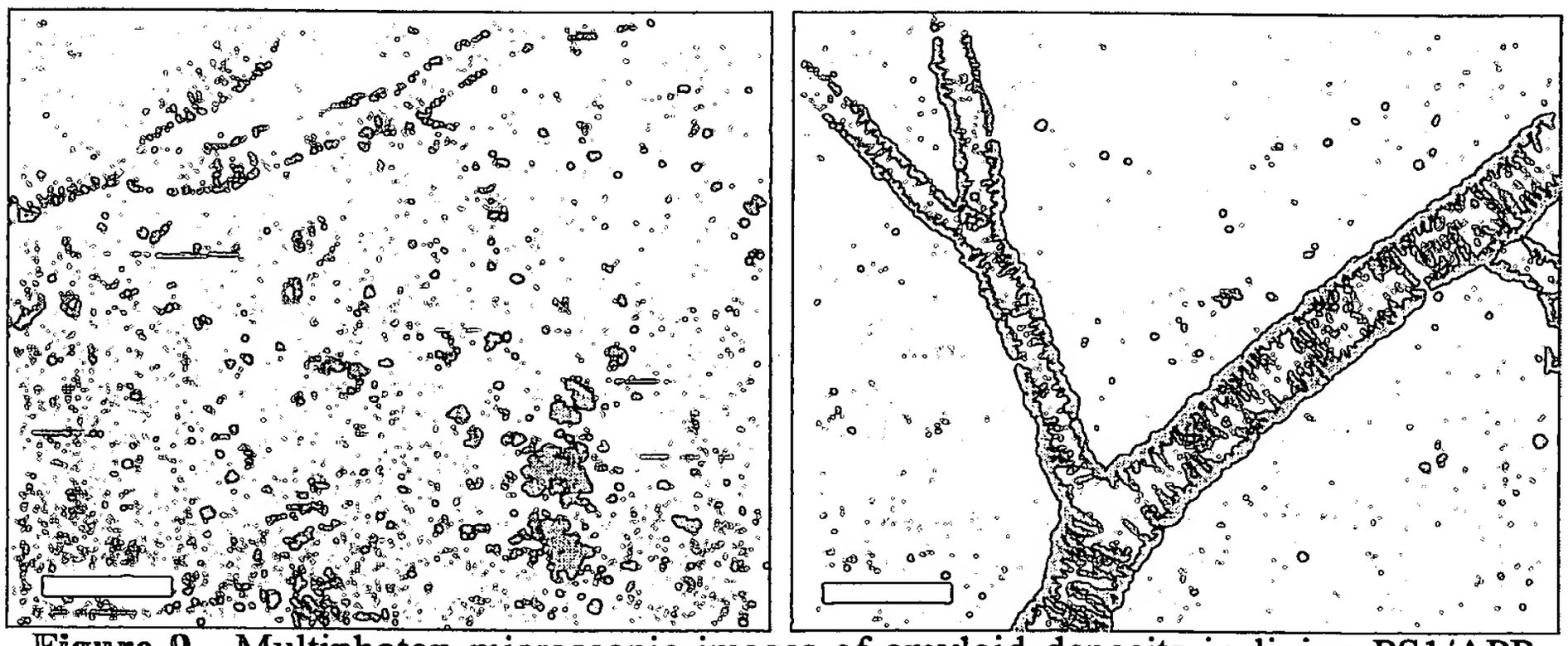

Figure 9. Multiphoton microscopic images of amyloid deposits in living PS1/APP mouse brain 24 h after ip injection of 10 mg/kg of BTA-1. These cortical images were obtained using a cortical window preparation slightly lateral to the sagittal suture and just posterior to the coronal suture. The views are projections ~300 μm deep and 615 x 615 μm square. The image on the left reveals several bright plaques in the lower, right portion of the panel and the faint outlines of cerebrovascular amyloid in the upper left portion of the panel. The image on the right shows a distinct amyloid-laden vessel. Note the absence of fluorescence emanating from within the vessels 24 h after the injection of BTA-1. The scale bar is 100 μm.